Polarized stimulated emission of 2D ensembles of plasmonic nanolasers

Nikita Toropov[1], Aisylu Kamalieva[2], Anton Starovoytov[1], Sajid Zaki[3], Tigran Vartanyan[1]*

Dr. Nikita Toropov, Dr. Anton Starovoytov, Prof. Tigran Vartanyan
[1]ITMO University, 49 Kronverkskiy pr., St. Petersburg, 197101, Russia

[2]Dr. Aisylu Kamalieva
CeramOptec SIA, DOMES Str., 1(a), Livani, LV-5316, Latvia

[3]Sajid Zaki
Aston Institute of Photonic Technologies, Aston University, Birmingham, B4 7ET, UK

E-mail: nikita.a.toropov@gmail.com

Keywords: nanoparticles, plasmons, organic thin films, stimulated emission, polarization, plasmonic nanolasers, spasers

Plasmonic nanolasers produce coherent light with wavelengths on a scale similar to their own or larger. In the past decade they have attracted intense interest, particularly from the emerging areas of integrated photonic circuits and biomedicine. Despite these capabilities, plasmonic nanolasers are still not completely understood, and this lack of understanding leads to confusing them with spasers and random lasers. Here, the operation of pure spaser-based plasmonic nanolaser arrays is presented. For this, a monolayer of silver nanoparticles (NPs) affixed to a dielectric surface and covered with a fluorescent PMMA–coumarin solid composite is investigated. The input–output characteristic measured for the composites on a bare substrate (without Ag nanoparticles) reveals that the emission at pump pulse energies above 2.4 mJ (at 355 nm excitation wavelength corresponding coumarin absorption) practically stops growing, instead inhibited by saturation. In contrast, in such structures with Ag nanoparticles an additional emission band pops up over a fluorescence background. It has a spectral width order of units of nanometers and its intensity grows faster than at lower pump pulse energies, revealing a nonlinear dependence of the input–output characteristic. The spaser-based lasing observed is completely linearly polarized and clearly directed as 45 degrees from the substrate.

This article has been accepted for publication and undergone full peer review but has not been through the copyediting, typesetting, pagination and proofreading process, which may lead to differences between this version and the Version of Record. Please cite this article as doi: 10.1002/adpr.202000083.

1. Introduction

The extensive development of nanoscale coherent optical sources is the current trend of research in the field of nanophotonics, directed towards the development of photonic integrated circuits capable of augmenting today's integrated electronic circuits.[1] The creation of nanometer-size lasers for the visible and infrared spectral ranges is impossible with traditional designs since the size of the resonator in a conventional laser cannot be smaller than its emission half-wavelength. This problem has been addressed by Bergman and Stockman[2] who suggested the new feedback mechanism in which the usual mirrors are replaced with metal nanostructures supporting localized plasmon oscillations. Similar to lasers, these devices were initially called 'spasers' and later termed 'plasmonic nanolasers',[2-9] which have been in focus for the last ten years.[10] Plasmonic nanolasers and spasers are commonly confused, but these two terms are not synonymous – spasers generate plasmons[2,11] while plasmonic nanolasers emit light[12] with wavelengths that are larger than their own sizes.

The plasmon-based sources overcome the diffraction limit, have faster (up to THz) switching capabilities in comparison to semiconductor counterparts, exploiting stimulated recombination,[13] limited to switching rates of the order of GHz. The spaser-based nanolaser is the smallest, biocompatible, and non-toxic tool, and can be incorporated in living tissues for a large number of biomedical *in vivo* and *in vitro* applications.[14-18] To date, several implementations of spasers and plasmonic nanolasers have been investigated: nanospheres,[12] nanodisks,[19] nanoflakes,[20] nanowires,[21] nanorods,[22] nanotori;[23] a topological spaser[11] and free electron excited spaser[24] were proposed. Organic dyes,[12] carbon nanostructures,[25] transition metal dichalcogenides,[26] as well as their hybrids[27,28] can act as a gain medium. The properties of subwavelength lasers are constantly improving; several groups have dealt with low-threshold for lasing,[29-32] multiwavelength lasing,[33] and high external quantum efficiency.[34] Despite the cogent results that spaser-based nanolaser have demonstrated, there are several negative responses to

plasmonic nanolasers, particularly because the lasing can be interpreted as a stimulated emission in a random laser[35,36] or as an amplified spontaneous emission.[37-43]

The first part of the experiment described in this article details plasmonic nanolasers and the reliability of different interpretations of their emission, as in conventional lasers. First, a lasing input–output characteristic has a threshold-like behavior. Second, it is characterized by a narrow emission band. Coherent optical sources can also have a distinguished polarization and directivity. For plasmon nanostructures, possibly enhanced-spontaneous radiation in an amplifying medium can cause spectral narrowing and, as a result, can be misinterpreted as stimulated emission. The presence of the spectral narrowing and nonlinear input-output dependence is not enough to interpret the results as the manifestation of spaser-based lasing. Therefore, it is necessary to study at least one of the characteristics of radiation, such as polarization, and we are aiming to take this into account in the second part of the work, as well as an analysis of radiation patterns of the emission. So, we propose plasmonic nanolasers based on a polymer–dye composite of 2D ensembles of silver nanoparticles where random lasing cannot be obtained. Silver nanoparticles in ensembles act as nanoresonators; a PMMA layer serves as a buffer layer preventing the uncontrolled fluorescence quenching of dye molecules by metals; dye molecules represent gain media. In contrast to previous studies, this work demonstrates a combination of the aforementioned lasing features. Thus, for the first time, the proposed ‘plaser’ implementation provides comprehensive evidence of the plasmonic nature of the stimulated emission.

2. Experimental section

2.1. Preparation of ensembles of silver nanoparticles with polymer–dye thin film

The laser dye coumarin 481 ($C_{14}H_{14}F_3NO_2$) was chosen as the gain medium because it has a high quantum yield of fluorescence, which is important to compensate for dissipation losses in the metallic resonators. The absorption and fluorescence spectra of this dye are well-overlapped with the Ag NPs plasmon resonance spectrum, a key factor to the implementation of the plasmonic-

based nanolaser. A coumarin dye layer was deposited on the surface of the samples with 2D ensembles of silver nanoparticles via the evaporation technique. The same layers were prepared on a clean quartz substrate to distinguish the NPs effect.

For the creation of 2D ensembles of plasmonic nanostructures, silver was chosen because among plasmonic materials in the spectral range investigated, it demonstrated minimal damping of plasmonic oscillations caused by losses. The physical vapor deposition technique in a vacuum chamber PVD-75 by 'Kurt J. Lesker' with a residual pressure level of ~10^{-7} Torr was used to obtain samples as granular films consisting of silver nanoparticles, with the equivalent thickness of 10 nm on quartz substrates. After, the samples were additionally thermally annealed at 220 °C. More details on the experimental setup, growing of nanoparticles and micrographs were given previously in refs.[44,45] and in Supporting Information. Using these micrographs and measuring the concentration of dye molecules dissolved from the surface, we estimated the surface density of plasmonic nanoparticles which has an order of 10^{10} cm^{-2}, their lateral sizes in average were of 60 nm in diameters with a big distribution, the thickness of dye layers, about 700 nm and the ratio of 2000 molecules per a nanoparticle. We considered that fluorophores located close to the metallic surface of NPs experience reducing or even are entirely quenched of their fluorescence.[46,47] Usually to minimize this effect, a dielectric layer can be used[47]. In this work we use a polymethyl methacrylate (PMMA) dielectric layer deposited on the surface of Ag NPs through the spin-coating technique. Following the work,[48] the thickness of PMMA layers was set to 10 nm.

2.2. Optical characterization of the prepared nanostructure

At first, all samples were characterized with absorption spectroscopy in the range of 300–700 nm. **Figure 1a** shows the optical density spectra of the coumarin thin film (line 1) 2D ensembles of Ag NPs (line 2), and hybrid structure, which consist of Ag NPs coated with the thin layer of PMMA and a coumarin layer on the top.

It is clearly seen that the hybrid structure possesses two absorption bands centered at the wavelength of 406 nm and 498 nm (Figure 1a). These two bands correspond to molecular and plasmonic absorption. The band with the maximum at the wavelength of 498 nm corresponds to the localized plasmon resonances of Ag NPs. Since the frequency of plasmonic oscillations depends on the dielectric permittivity of the environment, the resonances are red-shifted after PMMA and coumarin layers deposition. The band centered at 406 nm corresponds to molecular absorption of the thin film; the thin film spectrum is broader than a spectrum of this dye in a solution due to asymmetric interaction with the substrate. Due to near fields of plasmonic nanostructures the molecular absorption is also increased.

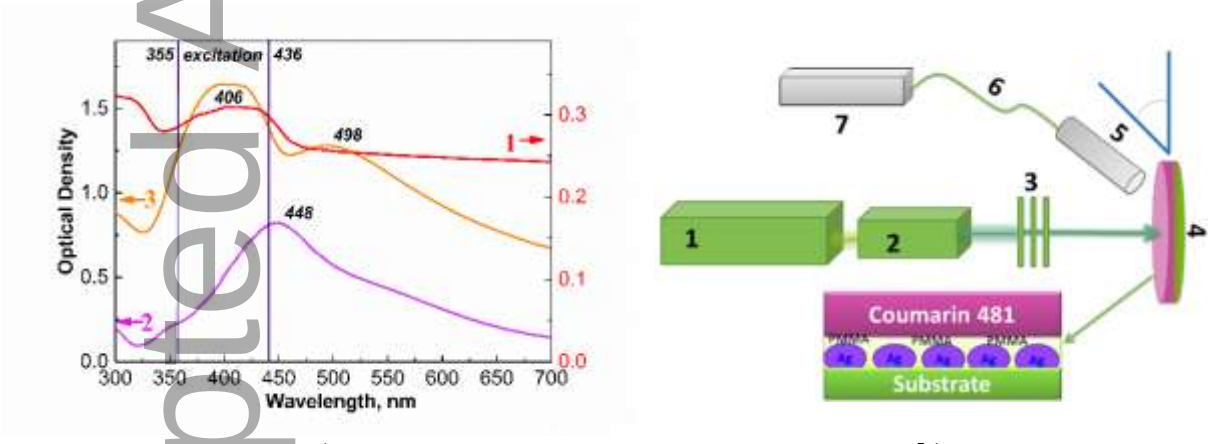

a) **b)**

Figure 1. (a) Optical density spectra of 1 – coumarin thin layer (right-hand scale), 2 – Ag NPs ensemble on the substrate, and 3 – hybrid of coumarin and Ag NPs. Vertical lines represent the spectral position of the optical pumping. (**b**) Emission registration scheme: 1 – Nd:YAG laser, 2 – third harmonic generator or optical parametric oscillator, 3 – attenuating filters, 4 – sample, 5 –fiber end with and without lenses, 7 –spectral analyzer Hamamatsu, connected to PC

These spectra were used to select excitation wavelengths. Excitation at 355 nm corresponds to minimal influence of plasmonic nanoparticles on the dye absorption, while excitation at 436 nm leads to considerable enhancement of dye absorption due to the overlapping of molecular and plasmonic bands.

2.3. Stimulated emission measurements

To register the input-output characteristics, the experimental scheme was assembled as schematically shown in Figure 1b. Optical pumping was provided by the Nd:YAG laser with a cascade of nonlinear converters: the third harmonic (355 nm) and optical parametric oscillator with the wavelength set to 436 nm. All measurements were performed with the laser operating in the pulsed mode: single pulses with a duration of 10 ns, the beam spot was 0.45 cm^2. The input energy was varied with neutral light filters and ranged from 0.3 mJ to 2.9 mJ (for 436 nm excitation) from 0.4 mJ to 9.4 mJ (for 355 nm excitation). We carefully checked the film was stable in the range of the excitation pulse energies (see Supporting Info). The emission signals from the samples were collected using the collimating lens and fed to the photonic multichannel analyzer Hamamatsu. In the experiments we conducted in the polarization investigation a dichroic polarizer was attached to the detecting system additionally. The emission of the samples was recorded at two mutually orthogonal positions of the polarizer, corresponding to *s*- and *p*- polarizations relative to the scattering plane. For the experiments on the radiation patterns investigation, an optical fiber with a small aperture connected to the photonic analyzer was used.

3. Results and discussion

3.1. Nonlinear input–output characteristic and spectral narrowing

Figure 2 plots the emission spectra of the coumarin thin films without (a) and with silver NPs (b) recorded at different pump energies and the excitation wavelength of 355 nm.

The dependences of the emission intensities of the coumarin dye layer and coumarin–PMMA on the top of Ag NPs on the pump pulse energy are shown in Figure 2c and 2d for both excitation wavelengths. First, we analyze Figure 2c (excitation at 355 nm). At pump energies below 1.1 mJ, the emission intensity, both for the coumarin layer on the substrate and the coumarin with silver NPs, grows equally linearly. Above the threshold energies of 1.1 mJ, both curves become sharply nonlinear, albeit in different sense. The dependence is sublinear for the bare coumarin layer,

namely because at pump pulse energies larger than 2.4 mJ, the input–output characteristic goes into saturation. Contrary to this, for the thin coumarin film with Ag NPs the emission continues to grow after the threshold. Its growth rapidly becomes much faster than at lower pump. The same behavior of the input–output characteristics was observed at 436 nm excitation. However, the threshold in this case was almost 2 times lower (0.6 mJ) due to the effect of spectral coincidence of coumarin and silver plasmonic bands.

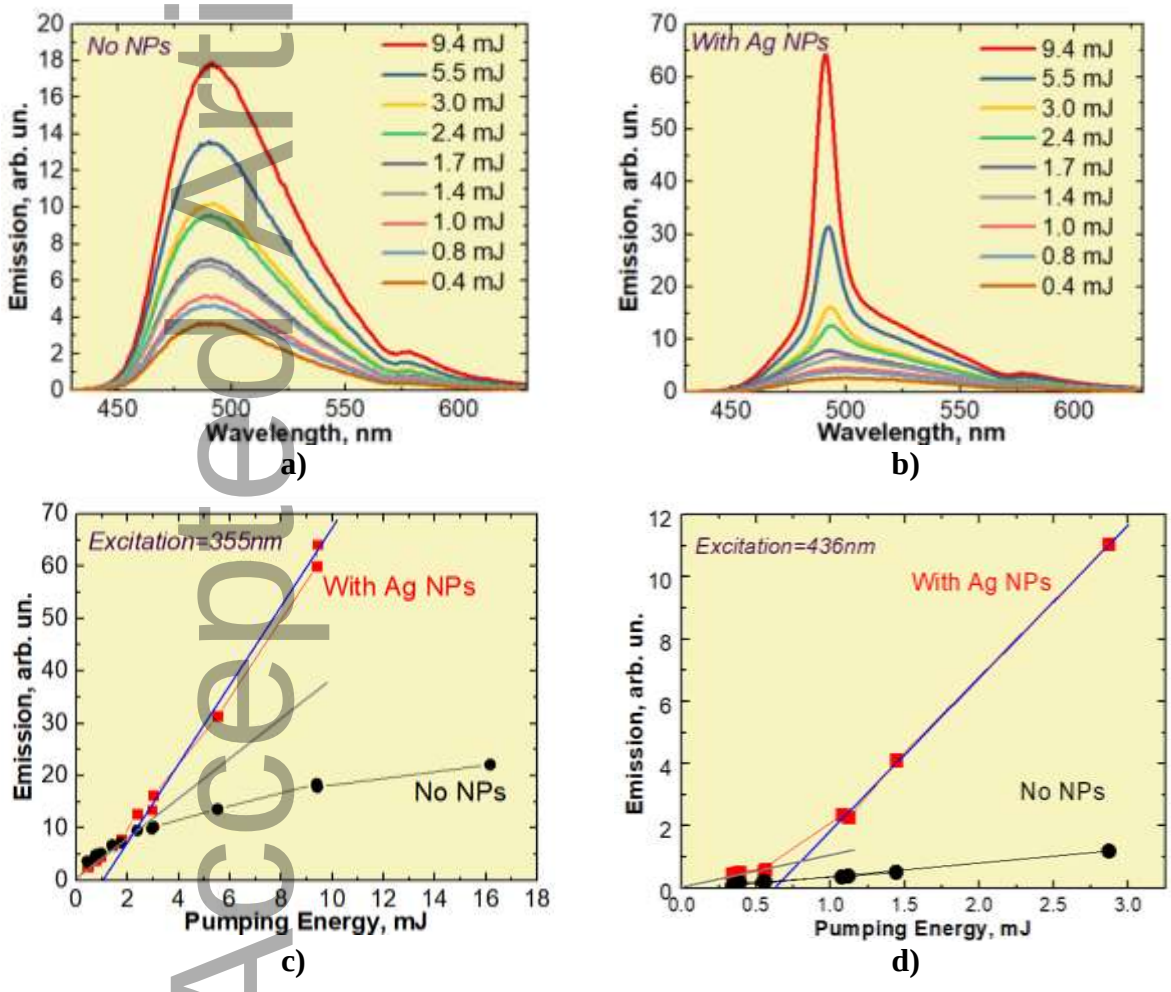

Figure 2. Emission spectra of the coumarin layers without (**a**) and with Ag NPs (**b**); (**c**) and (**d**) input–output characteristics of the emission depending on pumping energy of the coumarin layers with (red squares) and without (black dots) plasmonic nanoparticles (**c** – excitation at 355 nm; **d** – 436 nm). The blue and gray lines extrapolate pumping threshold and linear dependence of the emission at small pumping energies, correspondingly

All the emission spectra of the samples with Ag NPs measured at excitation levels above the threshold can be decomposed into two parts: the first part corresponds to the broad spectrum of a

fluorescence background. This part reproduces exactly the emission spectrum of the coumarin layer without Ag NPs. The second part is the narrow band emission, with the intensity growing faster than the background emission. This fact of narrowing the emission was clearly observed for both excitation wavelengths and only for the sample containing Ag NPs. The spectral width of the second part of the emission is larger in comparison with conventional lasers due to the broad distribution of shapes and sizes of nanoparticles.

It should be noted that in contrast to random lasers, the maximum intensity of the stimulated emission is independent of excitation wavelengths and remains constant, 491 nm.

3.2 Radiation pattern of the 2D ensembles of plasmonic nanoparticles with coumarin

The input–output characteristics plotted in Figure 2 were measured when the detector was positioned at 45 degrees from the substrate in the far field. For this, the detecting aperture was tilted at different angles from –60 to +60 degrees where the initial position of the detector was perpendicular to the exciting beam. The whole polar distribution of the angular variation of the intensity of the coumarin thin film with and without silver nanoparticles was not able to be measured because of weak signals, with the exception in this direction. According to well-known results,[49,50] the radiation pattern of a perpendicularly oriented dipole placed on a plane dielectric interface, is similar to that observed in our experiments. In particular, the absence of radiation in the direction parallel to the interface is in accord with the picture presented, by which the observed radiation is a sum of contributions of individual plasmonic nanolasers that act independently of each other. On the other hand, this observation contradicts all mechanisms that involve scattering of amplified radiation among many nanoparticles on a surface. Polarization measurements described in the next section further support the conclusion that plasmonic dipole sources are normally oriented to the surface.

3.3 Polarization of the stimulated emission

Another characteristic of the stimulated emission is polarization because spontaneous fluorescence is not polarized. We demonstrated above that the nonlinear dependence of the input–output characteristic and the spectral narrowing of the emission can be observed for plasmonic-based nanolasers. Similar results were analyzed in ref.,[51] about realizing directional random lasing, but we do not observe the same phenomenon when the PMMA–coumarin composite is excited. Moreover, it cannot demonstrate lasing since we observe the saturation of the emission.

For further proof of the stimulated nature of the radiation obtained from the hybrid nanostructure in this work, we also investigated its polarization. To this end, a dichroic polarizer was used. The emission signals of the samples were recorded at two positions of the polarizer (**Figure 3a**), corresponding to linear *s*- and *p*- polarizations relative to the scattering plane. With the polarizer in Position 1, corresponding to *s*-polarization (Figure 3b, blue curves), the emission spectrum has the usual shape, which is typical for a coumarin dye layer, while the narrow band described above disappears. The narrow fluorescence band of the hybrid film with Ag NPs is observed only with the polarizer in Position 2, corresponding to *p*-polarization (Figure 3b, orange curves).

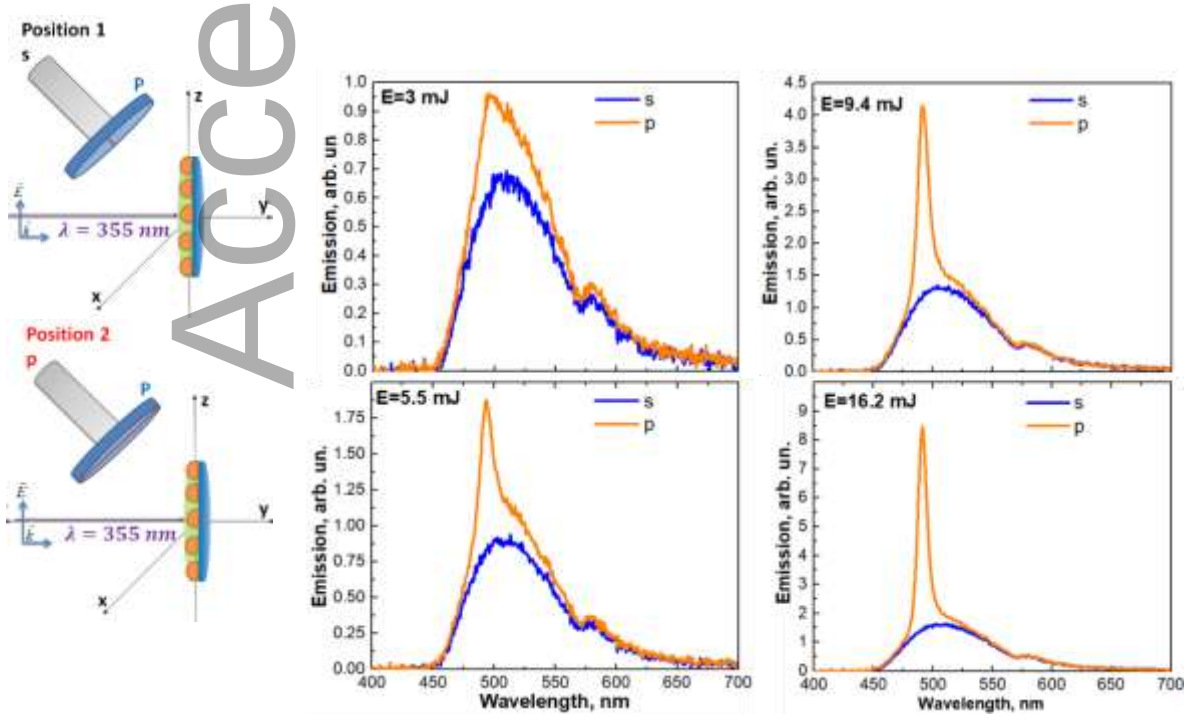

a) **b)**

Figure 3. (**a**) Schematic representation of the polarization measurements (P – polarizer) and (**b**) pairwise comparison of the emission of coumarin layers with Ag NPs at position 1 (blue spectra) and at position 2 (orange spectra)

In accord with the previously described results, the emission intensity of the structure with Ag NPs increases linearly under threshold pump energies, and continues to grow at larger pump energies with even larger rates than at lower pump energies if the polarizer is in Position 2. Contrary to that, if the polarizer is in Position 2, the fluorescence intensity at larger pump pulse energies goes into saturation. Analysis of these results shows that the stimulated emission radiation of the samples with Ag NPs are linearly polarized. That is to say, we show one more proof of the statement that the emission observed from the samples with silver nanoparticles is due to localized plasmon oscillations oriented perpendicular to the substrate surface.

4. Conclusion

We reliably demonstrated the stimulated emission of the 2D ensembles of plasmonic nanolasers, where the nanoscale layer of organic dye molecules acts as a gain medium and silver nanoparticles with sizes of ~10 nm arranged in the monolayer act as nanoresonators providing feedback. A set of stimulated emission features for these composites was ultimately measured and explained. The first signature of the stimulated origin of the emission is the nonlinear input–output characteristics obtained: at pump energies larger than 2.4 mJ a separate emission band over the wide fluorescence background appears in the spectra of the coumarin samples with silver nanoparticles; and grows faster than at lower pump energies. At the same time, the bare thin coumarin layer emission goes into saturation in the same range of pump energies. The second signature of the stimulated emission is the narrowness of its spectrum. The stimulated emission is linearly polarized in the scattering plane, while the fluorescence is unpolarized – the third signature of stimulated emission. The threshold of lasing is lower at pumping, with wavelengths corresponding to a better overlap of

molecular absorption bands and plasmonic oscillation frequencies. Finally, the radiation angular dependence shows the prominent direction of the stimulated radiation. Ultimately these features, combined with 2D geometry of the samples, negate interpretations of the emission based on random lasers or amplified spontaneous emission concepts. Thus, the results obtained put an end to many years of discussion about the nature of stimulated emission of the lasers with plasmonic nanostructures.

Supporting Information
Supporting Information is available from the Wiley Online Library.

Conflict of interest
The authors declare no conflict of interest.

Acknowledgements
This work was partially supported by the Council on grants of the President of the Russian Federation (MK-1984.2019.2) and the Government of Russia (08-08).

Received: ((will be filled in by the editorial staff))
Revised: ((will be filled in by the editorial staff))
Published online: ((will be filled in by the editorial staff))

References

[1] J. Khurgin, G. Sun, *Nature Photon.* **2014**, *8*, 468.

[2] D. J. Bergman, M. I. Stockman, *Phys. Rev. Lett.* **2003**, *90*, 027402.

[3] Y. Lu, J. Kim, H. Chen, C. Wu, N. Dabidian, C. E. Sanders, C. Wang, M. Lu, B. Li, X. Qiu, W. Chang, L. Chen, G. Shvets, C. Shih, S. Gwo, *Science* **2012**, *337*, 450.

[4] X. Meng, A. V. Kildishev, K. Fujita, K. Tanaka, V. M. Shalaev, *Nano Lett.* **2013**, *13*, 4106.

[5] K. G. Stamplecoskie, M. Grenier, J. C. Scaiano, *J. Am. Chem. Soc.* **2014**, *136*, 2956.

[6] V. M. Parfenyev, S. S. Vergeles, *Opt. Express*. **2014**, *22*, 13671.

[7] Y.-J. Lu, C.-Y. Wang, J. Kim, H.-Y. Chen, M.-Y. Lu, Y.-C. Chen, W.-H. Chang, L.-J. Chen, M. I. Stockman, C.-K. Shih, S. Gwo, *Nano Lett.* **2014**, *14*, 4381.

[8] S. Wang, X.-Y. Wang, B. Li, H.-Z. Chen, Y.-L. Wang, L. Dai, R. F. Oulton, R.-M. Ma, *Nat. Commun.* **2017**, *8*, 1889.

[9] P. Melentiev, A. Kalmykov, A. Gritchenko, A. Afanasiev, V. Balykin, A. S. Baburin, E. Ryzhova, I. Filippov, I. A. Rodionov, I. A. Nechepurenko, A. V. Dorofeenko, I. Ryzhikov, A. P. Vinogradov, A. A. Zyablovsky, E. S. Andrianov, A. A. Lisyansky, *Appl. Phys. Lett.* **2017**, *111*, 213104.

[10] S. I. Azzam, A. V. Kildishev, R.-M. Ma, C. Ning, R. Oulton, V. M. Shalaev, M. I. Stockman, J. Xu, X. Zhang, *Light Sci. Appl.*, **2020**, *9*, 90.

[11] J.-S Wu, V. Apalkov, M. I. Stockman, *Phys. Rev. Lett.* **2020**, *124*, 017701.

[12] M. A. Noginov, G. Zhu, A. M. Belgrave, R. Bakker, V. M. Shalaev, E. E. Narimanov, S. Stout, E. Herz, T. Suteewong, U. Wiesner, *Nature* **2009**, *460*, 1110.

[13] H. Wu, Y. X. Gao, P. Z. Xu, X. Guo, P. Wang, D. X. Dai, L. M. Tong, *Adv. Opt. Mater.* **2019**, *7*, 1900334.

[14] R. Ma, R. F. Oulton, *Nat. Nanotechnol.* **2019**, *14*, 12.

[15] E. I. Galanzha, R. Weingold, D. A. Nedosekin, M. Sarimollaoglu, J. Nolan, W. Harrington, A. S. Kuchyanov, R. G. Parkhomenko, F. Watanabe, Z. Nima, A. S. Biris, A. I. Plekhanov, M. I. Stockman, V. P. Zharov, *Nat. Commun.* **2017**, *8*, 15528.

[16] C. Alix-Panabières, K. Pantel, *Nat. Mater.* **2017**, *16*, 790.

[17] P. Song, J. Wang, M. Zhang, F. Yang, H. Lu, B. Kang, J. Xu, H. Chen. *Sci. Adv.* **2018**, *4*, eaat0292.

[18] Z. Gao, J. Wang, P. Song, B. Kang, J. Xu, H. Chen, *Adv. Mater.* **2020**, *32*, 1907233.

[19] C. Jayasekara, M. Premaratne, M. I. Stockman, S. D. Gunapala, *J. Appl. Phys.* **2015**, *118*, 173101.

[20] R.-M. Ma, R. F. Oulton, V. J. Sorger, G. Bartal, X. Zhang, *Nat. Mater.* **2011**, *10*, 110.

[21] R. F. Oulton, V. J. Sorger, T. Zentgraf, R.-M. Ma, C. Gladden, L. Dai, G. Bartal, X. Zhang, *Nature* **2009**, *461*, 629.

[22] M. T. Hill, M. Marell, E. S. P. Leong, B. Smalbrugge, Y. Zhu, M. Sun, P. J. van Veldhoven, E. J. Geluk, F. Karouta, Y.-S. Oei, R. Nötzel, C.-Z. Ning, M. K. Smit, *Opt. Express* **2009**, *17*, 11107.

[23] M. Khajavikhan, A. Simic, M. Katz, J. H. Lee, B. Slutsky, A. Mizrahi, V. Lomakin, Y. Fainman, *Nature* **2012**, *482*, 204.

[24] Y. Ye, F. Liu, K. Cui, X. Feng, W. Zhang, Y. Huang, *Opt. Express* **2018**, *26*, 31402.

[25] C. Rupasinghe, I. D. Rukhlenko, M. Premaratne, *ACS Nano* **2016**, *8*, 2431.

[26] C. Jayasekara, M. Premaratne, S. D. Gunapala, M. I. Stockman, *J. Appl. Phys.* **2016**, *119*, 133101.

[27] M. M. Tohari, A. Lyras, M. S. AlSalhi, *Nanomaterials (Basel)* **2020**, *10*, 416.

[28] L. Heng, L. Jhu-Hong, H. Kuo-Bin, Y. Min-Wen, C. Yi-Cheng, H. Chu-Yuan, Y. Jhen-Hong, C. Chang-Wei, H. Zhen-Ting, C. Kuo-Ping, L. Tzy-Rong, G. Shangjr, L. Tien-Chang, *Nano Lett.* **2019**, *19*, 50174.

[29] A. Fernandez-Bravo, D. Wang, E. S. Barnard, A. Teitelboim, C. Tajon, J. Guan, G. C. Schatz, B. E. Cohen, E. M. Chan, P. J. Schuck, T. W. Odom, *Nat. Mater.* **2019**, *18*, 1172.

[30] R. Ma, *Nat. Mater.* **2019**, *18*, 1152.

[31] C. Li, Z. Liu, J. Chen, Y. Gao, M. Li, Q. Zhang. *Nanophotonics*, **2019**, *8*, 2091.

[32] M. H. Motavas, A. Zarifkar, *Opt. Laser Technol.* **2019**, *111*, 315.

[33] D. Yuan, J. Wang, Y. Li, P. Ding, *J. Opt.* **2019**, *21*, 115001.

[34] S. Wang, H. Chen, R. Ma, *Nano Lett.* **2018**, *18*, 7942.

[35] W. Chen, J. Shiao, T. Tsai, D. Jiang, L. Chen, C. Chang, B. Lin, J. Lin, C. Kuo, *ACS Appl. Mater. Interfaces* **2020**, *12*, 2783.

[36] S. Chang, J. Wu, C. Kuo, S. Tsay, Y. Chen, J. Lin, *Opt. Lett.* **2020**, *45*, 5144.

[37] M. C. Gather, *Nat. Photon.* **2012**, *6*, 708.

[38] V. I. Balykin, *Phys. Usp.* **2018**, *61*, 846.

[39] M. Richter, M. Gegg, T. S. Theuerholz, A. Knorr, *Phys. Rev. B* **2015**, *91*, 035306.

[40] M. Premaratne, M. I. Stockman, *Adv. Opt. Photonics.* **2017**, *9*, 79.

[41] S. Li, L. Wang, T. Zhai, Z. Xu, Y. Wang, J. Wang, X. Zhang, *Opt. Express* **2015**, *23*, 23985.

[42] W. Z. W. Ismail, T. P. Vo, E. M. Goldys, J. M. Dawes, *Laser Phys.* **2015**, *25*, 085001.

[43] B. Guzelturk, Y. Kelestemur, M. Olutas, S. Delikanli, H. V. Demir, *ACS Nano* **2014**, *8*, 6599.

[44] N. A. Toropov, I. A. Gladskikh, P. S. Parfenov, T. A. Vartanyan, *Opt. Quant. Electron.* **2017**, *49*, 154.

[45] N. A. Toropov, N. B. Leonov, T. A. Vartanyan, *Phys. Status Solidi B* **2018**, *255*, 1700174.

[46] V. N. Pustovit, A. M. Urbas, A. V. Chipouline, T. V. Shahbazyan, *Phys. Rev. B,* **2016**, *93*, 165432.

[47] N. A. Toropov, A. N. Kamalieva, R. O. Volkov, E. P. Kolesova, D.-O. A. Volgina, S. A. Cherevkov, A. Dubavik, T. A. Vartanyan, *Opt. Laser Technol.* **2020**, *121*, 105821.

[48] C. B. Walsh, E. I. Franses, *Thin Solid Films* **2003**, *429*, 71.

[49] W. Lukosz, R. E. Kunz, *J. Opt. Soc. Am.* **1977**, *67*, 1607.

[50] W. Lukosz, R. E. Kunz, *J. Opt. Soc. Am.* **1997**, *67*, 1615.

[51] Z. Wang, X. Meng, X., A. V. Kildishev, A. Boltasseva, V. M. Shalaev, *Laser Photon Rev.* **2017**, *11*, 1700212.

The concept of plasmonic nanolasers is finally proven by investigation of the emission of thin polymer–dye films with and without 2D ensembles of silver nanoparticles. The threshold-like behavior of the input-output characteristic and spectral narrowing are clearly seen. In contrast to polymer–dye thin films emission, the stimulated emission obtained is linearly polarized.

Aisylu Kamalieva, Anton Starovoytov, Sajid Zaki, Tigran Vartanyan, Nikita Toropov* (corresponding author)

Polarized stimulated emission of 2D ensembles of plasmonic nanolasers